- Ion mobility–mass spectrometry of a rotary ATPase reveals ATP-induced reduction in conformational flexibility
  Zhou, M.; Politis, A.; Davies, R. B. ; Liko, I.; Wu, K.-J.; Stewart, A. G.; Stock, D.; Robinson, C. V. *Nature Chem.* **2014**, *6*, 208–215.
  Abstract:

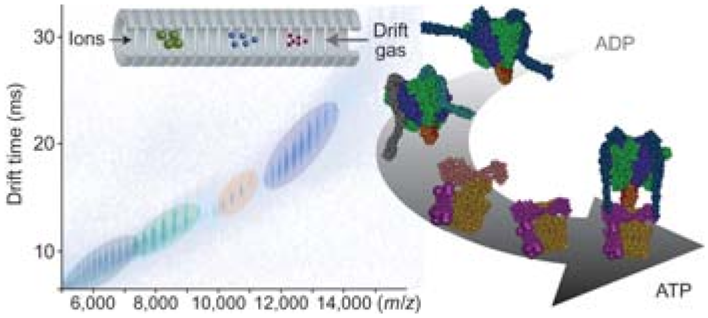

Rotary ATPases play fundamental roles in energy conversion as their catalytic rotation is associated with interdomain fluctuations and heterogeneity of conformational states. Using ion mobility mass spectrometry we compared the conformational dynamics of the intact ATPase from Thermus thermophilus with those of its membrane and soluble subcomplexes. Our results define regions with enhanced flexibility assigned to distinct subunits within the overall assembly. To provide a structural context for our experimental data we performed molecular dynamics simulations and observed conformational changes of the peripheral stalks that reflect their intrinsic flexibility. By isolating complexes at different phases of cell growth and manipulating nucleotides, metal ions and pH during isolation, we reveal differences that can be related to conformational changes in the Vo complex triggered by ATP binding. Together these results implicate nucleotides in modulating flexibility of the stator components and uncover mechanistic detail that underlies operation and regulation in the context of the holoenzyme.

- Conversion of light into macroscopic helical motion
  Iamsaard, S.; Aßhoff, S. J.; Matt, B.; Kudernac, T.; Cornelissen, J. J. L. M.; Fletcher, S. P.; Katsonis, N. *Nature Chem.* **2014**, *6*, 229–235.
  Abstract:

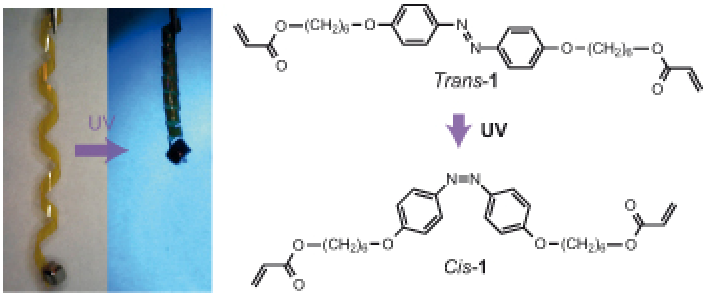

A key goal of nanotechnology is the development of artificial machines capable of converting molecular movement into macroscopic work. Although conversion of light into shape changes has been reported and compared to artificial muscles, real applications require work against an external load. Here, we describe the design, synthesis and operation of spring-like materials capable of converting light energy into mechanical work at the macroscopic scale. These versatile materials consist of molecular switches embedded in liquid-crystalline polymer springs. In these springs, molecular movement is converted and amplified into controlled and reversible twisting motions. The springs display complex motion, which includes winding, unwinding and helix inversion, as dictated by their initial shape. Importantly, they can produce work by moving a macroscopic object and mimicking mechanical movements, such as those used by plant tendrils to help the plant access sunlight. These functional materials have potential applications in micromechanical systems, soft robotics and artificial muscles.

- Controlling a Polymer Adhesive Using Light and a Molecular Switch
  Asadirad, A. M.; Boutault, S.; Erno, Z.; Branda, N. R. *J. Am. Chem. Soc*. **2014**, *136*, 3024-3027.
  Abstract:

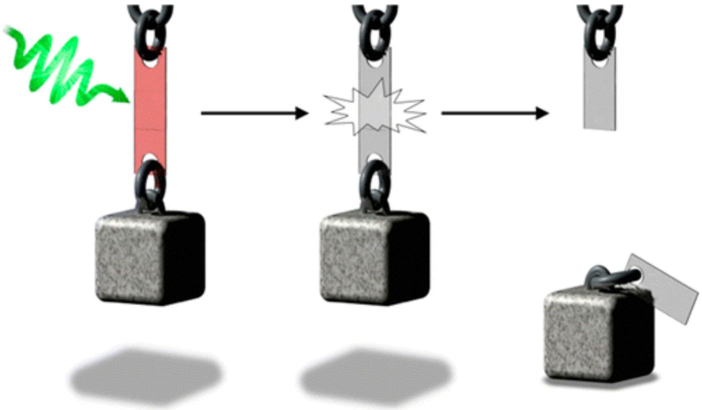

A thermally remendable polymer was synthesized by the Diels–Alder reaction between dithienylfuran and maleimide monomers to generate a photoresponsive diarylethene. UV light (312 nm) and visible light (>435 nm) “gate” the reversibility of the Diels–Alder reaction and turn the self-healing properties of the polymer “off” and “on”, respectively. After exposure to UV light, the strength of the polymer as an adhesive is enhanced. Visible light weakens the adhesive.

- Control of Surface Wettability Using Tripodal Light-Activated Molecular Motors
  Chen, K.-Y.; Ivashenko, O.; Carroll, G. T.; Robertus, J.; Kistemaker, J. C. M.; London, G.; Browne, W. R.; Rudolf, P.; Feringa, B. L. *J. Am. Chem. Soc*. **2014**, *136*, 3219-3224.
  Abstract:

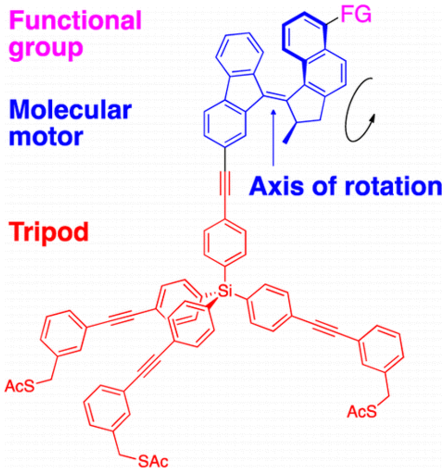

Monolayers of fluorinated light-driven molecular motors were synthesized and immobilized on gold films in an altitudinal orientation via tripodal stators. In this design the functionalized molecular motors are not interfering and preserve their rotary function on gold. The wettability of the self-assembled monolayers can be modulated by UV irradiation.

- Coupled Nanomechanical Motions: Metal-Ion-Effected, pH-Modulated, Simultaneous Extension/Contraction Motions of Double-Domain Helical/Linear Molecular Strands
  Stadler, A.-M.; Lehn, J.-M. *J. Am. Chem. Soc.* **2014**, *136*, 3400–3409.
  Abstract:

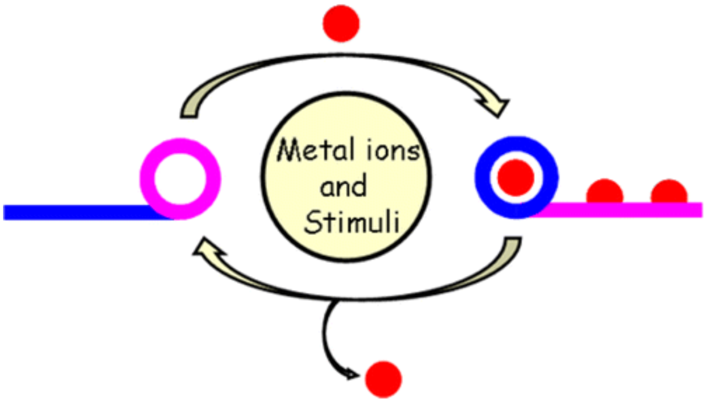

A new class of shape-enforced synthetic polyheterocyclic molecular strands, containing both a helical and a linear domain, has been designed and synthesized. On reaction with Pb(II), under the effect of cation binding to the coordination subunits, the helical section unfolds into a linear shape in the complex and the linear domain folds into a helical ligand wrapped around the bound cations. Such double-domain ligand strands are thus able to undergo a combined unfolding–folding interconversion on binding and release of metal cations. These changes can be modulated through coupling to a competing ligand that reversibly binds and releases metal cations, when respectively unprotonated and protonated, on effecting alternate pH changes. The resulting process thus performs nanomechanical extension/contraction molecular motions of a linear motor type, which is fueled by acid–base neutralization.

- Quantitative Bimolecular Recombination in Organic Photovoltaics through Triplet Exciton Formation
  Chow, P. C. Y.; Gélinas, S.; Rao, A.; Friend, R. H. *J. Am. Chem. Soc.* **2014,** *136*, 3424–3429.
  Abstract:

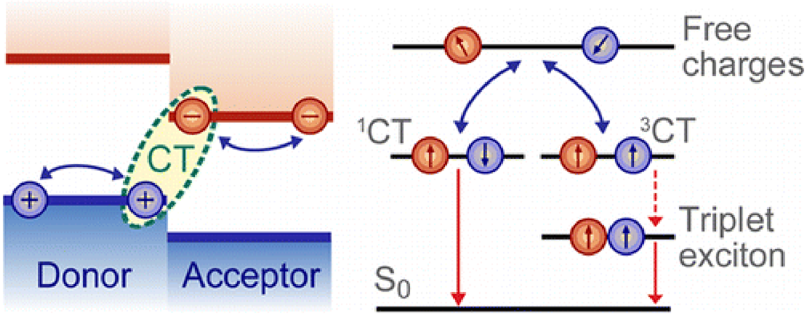

The nanoscale morphology and high charge densities in organic photovoltaics (OPVs) lead to a high rate of bimolecular encounters between spin-uncorrelated electrons and holes. This process can lead to the formation of low-energy triplet excitons on the donor polymer that decay nonradiatively and limit the device performance. We use time-resolved optical spectroscopy to characterize the effect of morphology through the use of solvent additives such as 1,8-octanedithiol (ODT) on triplet dynamics and charge recombination in blends of poly[2,6-(4,4-bis(2-ethylhexyl)-4H-cyclopenta[2,1-b;3,4-b′]-dithiophene)-alt-4,7-(2,1,3-benzothiadiazole)] and [6,6]-phenyl-C71-butyric acid methyl ester. This is an attractive OPV system since the extended absorption of the polymer into the near-infrared gives good coverage of the solar spectrum, but nevertheless, the internal quantum efficiency (IQE) has not been reported to be higher than 65% under short circuit conditions. We find that, without ODT, the IQE is 48% and 16% of excitations decay via bimolecular triplet formation. With ODT treatment, which improves crystallinity and carrier mobility, the IQE increases to 65%, but bimolecular triplet formation significantly increases and now accounts for all of the recombination (35% of charges).

- *Kinetically controlled phenomena in dynamic combinatorial libraries*
  Ji, Q.; Liraga, R. C.; Miljanić, O. Š. *Chem. Soc. Rev.* **2014**, *43*, 1873-1884.
  Abstract:

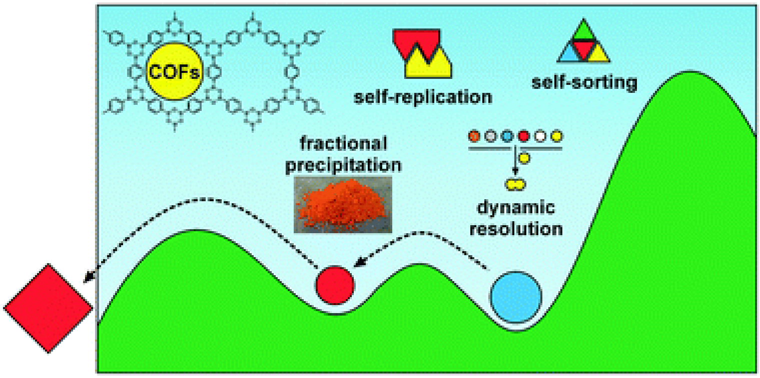

Dynamic combinatorial libraries (DCLs) are collections of structurally related compounds that can interconvert through reversible chemical reaction(s). Such reversibility endows DCLs with adaptability to external stimuli, as rapid interconversion allows quick expression of those DCL components which best respond to the disturbing stimulus. This Tutorial Review focuses on the kinetically controlled phenomena that occur within DCLs. Specifically, it will describe dynamic chiral resolution of DCLs, their self-sorting under the influence of irreversible chemical and physical stimuli, and the autocatalytic behaviours within DCLs which can result in self-replicating systems. A brief discussion of precipitation-induced phenomena will follow and the review will conclude with the presentation of covalent organic frameworks (COFs)—porous materials whose synthesis critically depends on the fine tuning of the crystal growth and error correction rates within large DCLs.

- Self-assembled coordination cages based on banana-shaped ligands
  Han, M.; Engelhard, D. M.; Clever, G. H. *Chem. Soc. Rev.* **2014**, *43*, 1848-1860.
  Abstract:

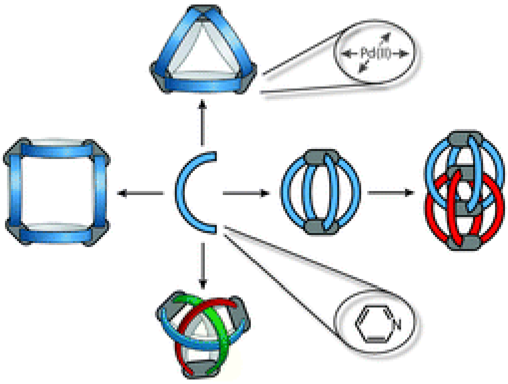

The combination of pyridyl ligands and square-planar Pd(II) or Pt(II) cations has proven to be a very reliable recipe for the realization of supramolecular self-assemblies. This tutorial review deals with the design, synthesis and host–guest chemistry of discrete coordination cages built according to this strategy. The focus is set on structures obeying the formula [Pd_nL_{2n}] (n = 2–4). The most discussed ligands are bent, bis-monodentate bridges having their two donor sites pointing in the same direction. The structures of the resulting cages range from simple globules over intertwined knots to interpenetrated dimers featuring three small pockets instead of one large cavity. The cages have large openings that allow small guest molecules to enter and leave the cavities. Most structures are cationic and thus favour the uptake of anionic guests. Some examples of host–guest complexes are discussed with emphasis on coencapsulation and allosteric binding phenomena. Aside from cages in which the ligands have only a structural role, some examples of functional ligands based on photo- and redox-active backbones are presented.

- MALDI–TOF Mass Spectrometry of Polyphenylene Dendrimers up to the Megadalton Range. Elucidating Structural Integrity of Macromolecules at Unrivaled High Molecular Weights
  Räder, H. J.; Nguyen, T.-T.-T.; Müllen, K. *Macromolecules* **2014**, *47*, 1240–1248.
  Abstract:

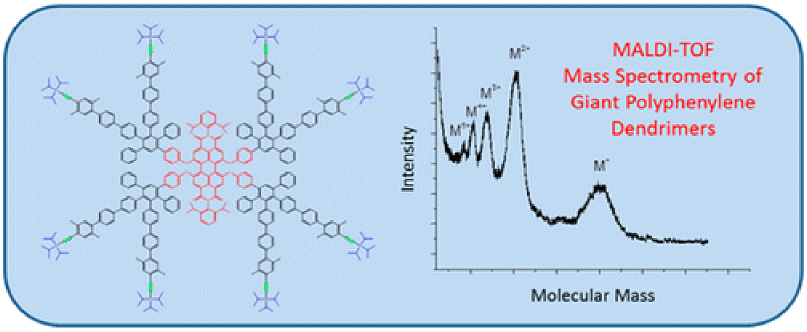

A complete homologous series of polyphenylene dendrimers up to the ninth generation (G9) corresponding to a theoretical molecular weight of 1.9 MDa was characterized by MALDI–TOF mass spectrometry. Mass spectrometry of synthetic polymers at extreme high masses is still uncommon to date and the underlying probable reasons are discussed. The measurements provided insight into the structural integrity, especially for the highest generations which could not be obtained by standard analytical tools for polymer characterization, such as gel permeation chromatography. The degree of structural integrity was elucidated by comparison of the measured molecular weights with theoretical molecular weights, calculated for the perfect structures. As a result, the dendrimers own structural perfection up to G4 and show increasing deviations with each higher generation starting at G5. The deviations could be partially attributed to a systematic error of the measurements but mainly to an increasing number of missing branches inside the dendrimers. The detected changes within the homologues series were discussed with respect to polymer-chemical aspects of the divergent route of dendrimer synthesis. Overall the whole dendrimer series shows very narrow polydispersity values below 1.005 which confirm the high structural integrity of these giant molecules up to a diameter of 33 nm, which can be considered as molecularly defined nanosized particles.

- Formation of Tetragonally-Packed Rectangular Cylinders from ABC Block Terpolymer Blends
  Asai, Y.; Yamada, K.; Yamada, M.; Takano, A.; Matsushita, Y. *ACS Macro Lett.* **2014**, *3*, 166–169.
  Abstract:

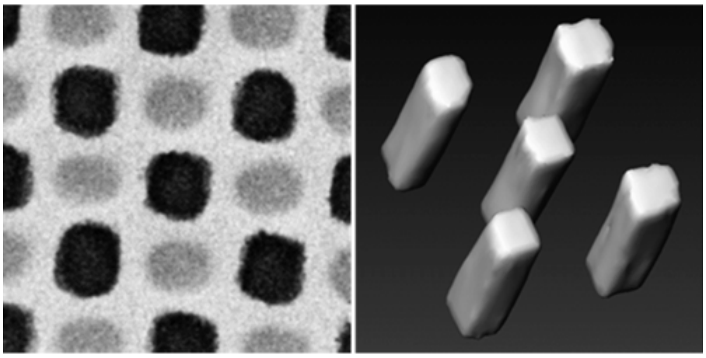

Effect of composition distribution of ABC linear terpolymers on the formation of periodic structures was investigated. Five poly(isoprene-*b*-styrene-*b*-2-vinylpyridine) (ISP) triblock terpolymers with almost constant molecular weights of ca. 130k and with similar center-block fraction at around 0.55, were blended variously. It has been found that tricontinuous gyroid structures gradually transform into a cylindrical structure whose rectangular cylinders are packed tetragonally if composition distribution increases. Further experiments by 3D-TEM observation on binary equimolar mixtures of two molecules with similar molecular weights of 122k and 124k, giving the average composition of $\phi_I/\phi_S/\phi_P$ = 0.23/0.59/0.18, has verified to show more evident rectangular-shaped cylinders with 4-fold symmetry. This new structure, having periodic surfaces with nonconstant mean-curvature, could be formed due to the systematic localization of component polymer chains along the domain interfaces.

- Thermoresponsive PNIPAAM bottlebrush polymers with tailored side-chain length and end-group structure
  Li, X.; ShamsiJazeyi, H.; Pesek, S. L.; Agrawal, A.; Hammouda, B.; Verduzco, R. *Soft Matter* **2014**, *10,* 2008-2015.
  <u>Abstract:</u>

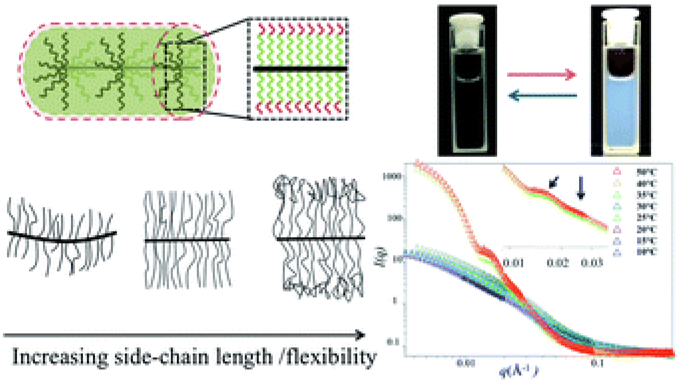

We explore the phase behaviour, solution conformation, and interfacial properties of bottlebrush polymers with side-chains comprised of poly(N-isopropylacrylamide) (PNIPAAM), a thermally responsive polymer that exhibits a lower critical solution temperature (LCST) in water. PNIPAAM bottlebrush polymers with controlled side-chain length and side-chain end-group structure are prepared using a "grafting-through" technique. Due to reduced flexibility of bottlebrush polymer side-chains, side-chain end-groups have a disproportionate effect on bottlebrush polymer solubility and phase behaviour. Bottlebrush polymers with a hydrophobic end-group have poor water solubilities and depressed LCSTs, whereas bottlebrush polymers with thiol-terminated side-chains are fully water-soluble and exhibit an LCST greater than that of PNIPAAM homopolymers. The temperature-dependent solution conformation of PNIPAAM bottlebrush polymers in D2O is analyzed

by small-angle neutron scattering (SANS), and data analysis using the Guinier–Porod model shows that the bottlebrush polymer radius decreases as the temperature increases towards the LCST for PNIPAAM bottlebrush polymers with relatively long 9 kg mol^{-1} side-chains. Above the LCST, PNIPAAM bottlebrush polymers can form a lyotropic liquid crystal phase in water. Interfacial tension measurements show that bottlebrush polymers reduce the interfacial tension between chloroform and water to levels comparable to PNIPAAM homopolymers without the formation of microemulsions, suggesting that bottlebrush polymers are unable to stabilize highly curved interfaces. These results demonstrate that bottlebrush polymer side-chain length and flexibility impact phase behavior, solubility, and interfacial properties.

- Mechanics of biological networks: from the cell cytoskeleton to connective tissue
  Pritchard, R. H.; Huang, Y. Y. S.; Terentjev, E. M. *Soft Matter* **2014***, 10,* 1864-1884.
  Abstract:

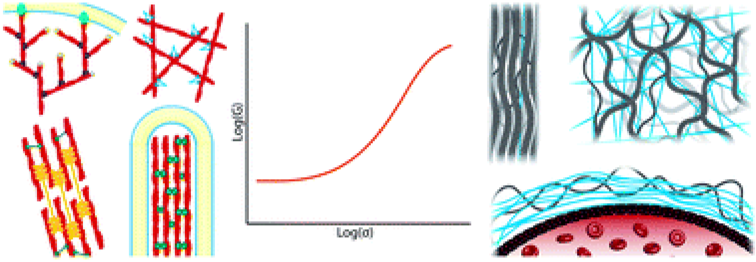

From the cell cytoskeleton to connective tissues, fibrous networks are ubiquitous in metazoan life as the key promoters of mechanical strength, support and integrity. In recent decades, the application of physics to biological systems has made substantial strides in elucidating the striking mechanical phenomena observed in such networks, explaining strain stiffening, power law rheology and cytoskeletal fluidisation – all key to the biological function of individual cells and tissues. In this review we focus on the current progress in the field, with a primer into the basic physics of individual filaments and the networks they form. This is followed by a discussion of biological networks in the context of a broad spread of recent in vitro and in vivo experiments.

- Self-Assembly Enhances the Strength of Fibers Made from Vimentin Intermediate Filament Proteins
  Pinto, N.; Yang, F.-C.; Negishi, A.; Rheinstädter, M. C.; Gillis, T. E.; Fudge, D. S. *Biomacromolecules* **2014**, *15*, 574–581.
  Abstract:

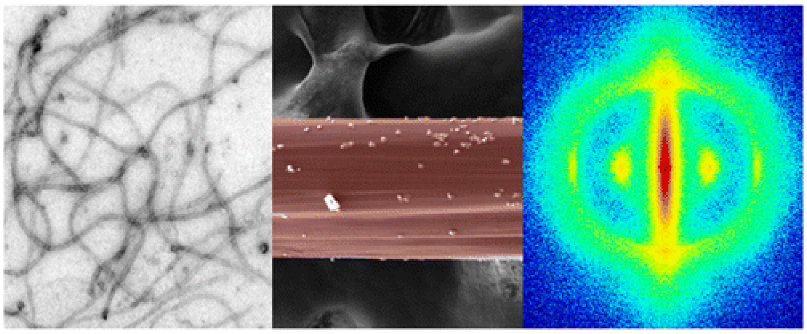

Hagfish slime threads were recently established as a promising biomimetic model for efforts to produce ecofriendly alternatives to petroleum polymers. Initial attempts to make fibers from solubilized slime thread proteins fell short of achieving the outstanding mechanics of native slime

threads. Here we tested the hypothesis that the high strength and toughness of slime threads arise from the ability of constituent intermediate filaments to undergo a stress-induced α-to-β transition. To do this, we made fibers from human vimentin proteins that were first allowed to self-assemble into 10 nm intermediate filaments. Fibers made from assembled vimentin hydrogels underwent an α-to-β transition when strained and exhibited improved mechanical performance. Our data demonstrate that it is possible to make materials from intermediate filament hydrogels and that mimicking the secondary structure of native hagfish slime threads using intermediate filament self-assembly is a promising strategy for improving the mechanical performance of biomimetic protein materials.

- Light-Responsive Micelles of Spiropyran Initiated Hyperbranched Polyglycerol for Smart Drug Delivery
  Son, S.; Shin, E.; Kim, B.-S. *Biomacromolecules* **2014**, *15*, 628–634.
  Abstract:

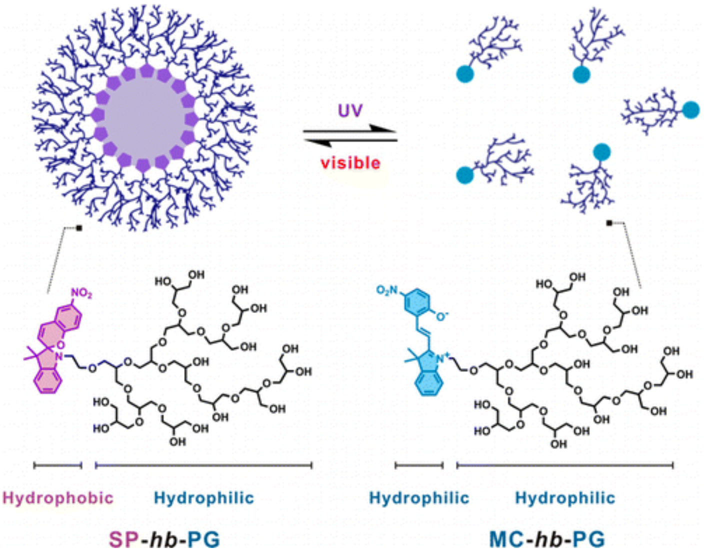

Light-responsive polymeric micelles have emerged as site-specific and time-controlled systems for advanced drug delivery. Spiropyran (SP), a well-known photochromic molecule, was used to initiate the ring-opening multibranching polymerization of glycidol to afford a series of hyperbranched polyglycerols (SP-*hb*-PG). The micelle assembly and disassembly were induced by an external light source owing to the reversible photoisomerization of hydrophobic SP to hydrophilic merocyanine (MC). Transmission electron microscopy, atomic force microscopy, UV/vis spectroscopy, and dynamic light scattering demonstrated the successful assembly and disassembly of SP-*hb*-PG micelles. In addition, the critical micelle concentration (CMC) was determined through the fluorescence analysis of pyrene to confirm the amphiphilicity of respective SP-*hb*-PG$_n$ (n = 15, 29, and 36) micelles, with CMC values ranging from 13 to 20 mg/L, which is correlated to the length of the polar polyglycerol backbone. Moreover, the superior biocompatibility of the prepared SP-*hb*-PG was evaluated using WI-38 cells and HeLa cells, suggesting the prospective applicability of the micelles in smart drug delivery systems.

- Rational design of fluorescent light-up probes based on an AIE luminogen for targeted intracellular thiol imaging
  Yuan, Y.; Kwok, R. T. K.; Feng, G.; Liang, J.; Geng, J.; Tang, B. Z.; Liu, B. *Chem. Commun.* **2014***, 50,* 295-297.

Abstract:

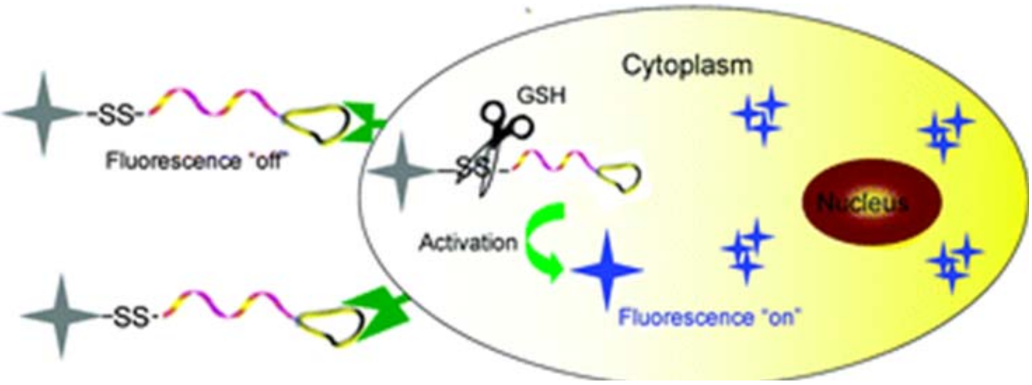

A water-soluble fluorescent light-up bioprobe based on a luminogen with aggregation-induced emission characteristics was developed for targeted intracellular thiol imaging.

- A pillar [5] arene/imidazolium [2]rotaxane: solvent- and thermo-driven molecular motions and supramolecular gel formation
  Dong, S.; Yuan, J.; Huang, F. *Chem. Sci.* **2014**, *5,* 247-252.
  Abstract:

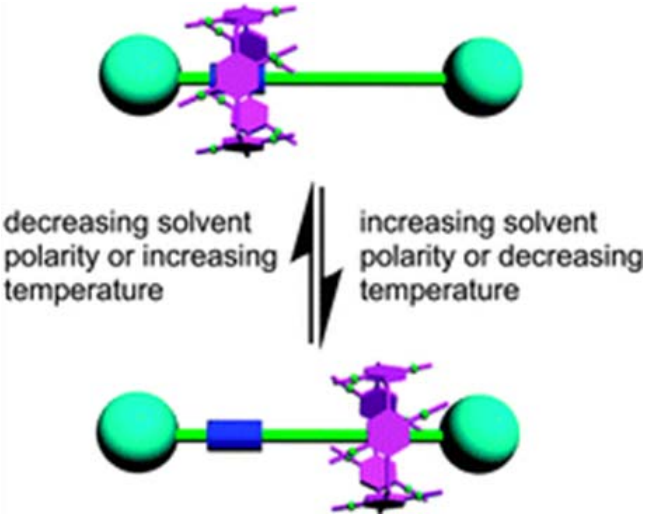

Based on the pillar [5]arene/imidazolium recognition motif, a [2]rotaxane was effectively prepared. Solvent/temperature triggered molecular motions of the pillar[5]arene ring on the imidazolium axle were successfully realized. By comparison of proton NMR spectra of the [2]rotaxane in different solvents, we found that if we increased the solvent polarity, the pillar[5]arene ring by changing the temperature. Furthermore, in DMSO, the [2]rotaxane self-assembled to form a supramolecualr gel, which showed multiple stimuli-responsiveness.

- Sacrificial-Post Templating Method for Block Copolymer Self-Assembly
  Tavakkoli, K. G. A.; Nicaise, S. M.; Hannon, A. F.; Gotrik, K. W.; Alexander-Katz, A.; Ross, C. A.; Berggren, K. K. *Small* **2014**, *3*, 493-499.
  Abstract:

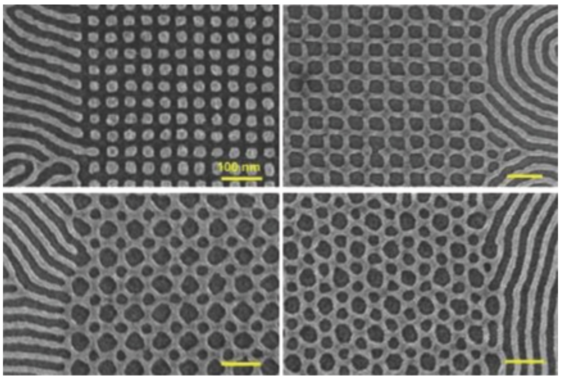

A sacrificial-post templating method is presented for directing block copolymer self-assembly to form nanostructures consisting of monolayers and bilayers of microdomains. In this approach, the topographical post template is removed after self-assembly and therefore is not incorporated into the final microdomain pattern. Arrays of nanoscale holes of different shapes and symmetries, including mesh structures and perforated lamellae with a bimodal pore size distribution, are produced. The ratio of the pore sizes in the bimodal distributions can be varied via the template pitch, and agrees with predictions of self consistent field theory.

- Size Controlled Synthesis of Silicon Nanocrystals Using Cationic Surfactant Templates
  Linehan, K.; Doyle, H. *Small* **2014**, *3*, 584-590.
  Abstract:

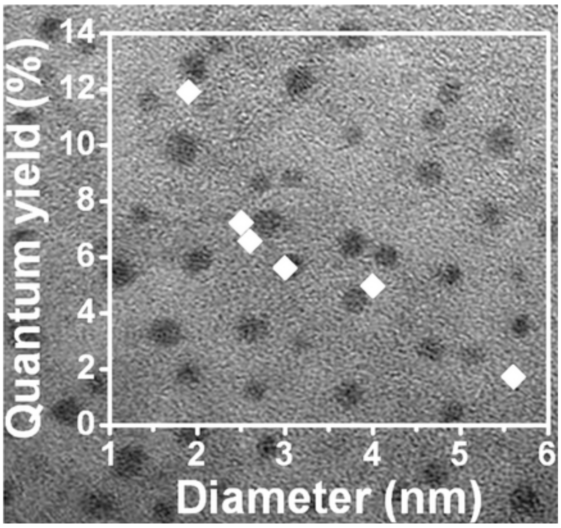

Alkyl-terminated silicon nanocrystals (Si NCs) are synthesized at room temperature by hydride reduction of silicon tetrachloride ($SiCl_4$) within inverse micelles. Highly monodisperse Si nanocrystals with average diameters ranging from 2 to 6 nm are produced by variation of the cationic quaternary ammonium salts used to form the inverse micelles. Transmission electron microscopy imaging shows that the NCs are highly crystalline, while FTIR spectra confirm that the NCs are passivated by covalent attachment of alkanes, with minimal surface oxidation. UV-vis absorbance and photoluminescence spectroscopy show significant quantum confinement effects, with moderate absorption in the UV spectral range, and a strong blue emission with a marked dependency on excitation wavelength. The photoluminescence quantum yield (Φ) of the Si NCs exhibits an inverse relationship with the mean NC diameter, with a maximum of 12% recorded for 2 nm NCs.

- Toward a Symphony of Reactivity: Cascades Involving Catalysis and Sigmatropic Rearrangements
  Jones, A. C.; May, J. A.; Sarpong, R.; Stoltz, B. M. *Angew. Chem. Int. Ed*. **2014**, *53*, 2556–2591.
  Abstract:

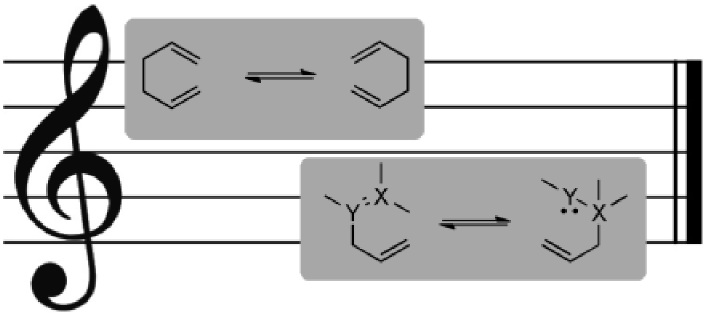

Catalysis and synthesis are intimately linked in modern organic chemistry. The synthesis of complex molecules is an ever evolving area of science. In many regards, the inherent beauty associated with a synthetic sequence can be linked to a certain combination of the creativity with which a sequence is designed and the overall efficiency with which the ultimate process is performed. In synthesis, as in other endeavors, beauty is very much in the eyes of the beholder. It is with this in mind that we will attempt to review an area of synthesis that has fascinated us and that we find extraordinarily beautiful, namely the combination of catalysis and sigmatropic rearrangements in consecutive and cascade sequences.

- Copolymerization of Metal Nanoparticles: A Route to Colloidal Plasmonic Copolymers
  Liu, K.; Lukach, A.; Sugikawa, K.; Chung, S.; Vickery, J.; Therien-Aubin, H.; Yang, B.; Rubinstein, M.; Kumacheva, E. *Angew. Chem. Int. Ed.* **2014**, *53*, 2648–2653.
  Abstract:

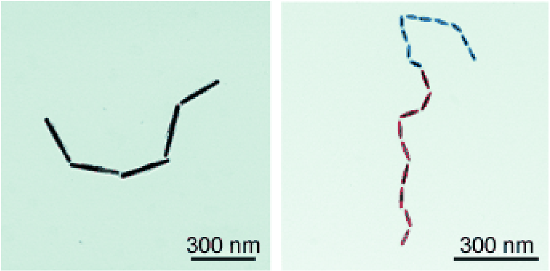

The resemblance between colloidal and molecular polymerization reactions is very useful in fundamental studies of polymerization reactions, as well as in the development of new nanoscale systems with desired properties. Future applications of colloidal polymers will require nanoparticle ensembles with a high degree of complexity that can be realized by hetero-assembly of NPs with different dimensions, shapes, and compositions. A method has been developed to apply strategies from molecular copolymerization to the co-assembly of gold nanorods with different dimensions into random and block copolymer structures (plasmonic copolymers). The approach was extended to the co-assembly of random copolymers of gold and palladium nanorods. A kinetic model validated and further expanded the kinetic theories developed for molecular copolymerization reactions.

- Photocontrol Over Self-Assembled Nanostructures of π–π Stacked Dyes Supported by the Parallel Conformer of Diarylethene
  Yagai, S.; Iwai, K.; Yamauchi, M.; Karatsu, T.; Kitamura, A.; Uemura, S.; Morimoto, M.; Wang, H.; Würthner, F. *Angew. Chem. Int. Ed.* **2014**, *53*, 2602–2606.

Abstract:

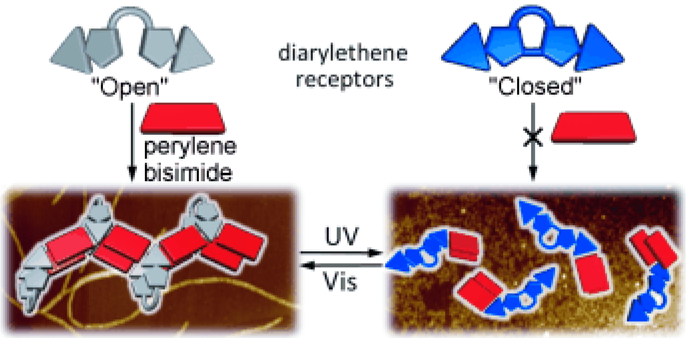

Diarylethenes (DAEs) have rarely been used in the design of photoresponsive supramolecular assemblies with a well-defined morphology transition owing to rather small structural changes upon photoisomerization. A supramolecular design based on the parallel conformation of DAEs enables the construction of photoresponsive dye assemblies that undergo remarkable nanomorphology transitions. The cooperative stacking of perylene bisimide (PBI) dyes was used to stabilize the parallel conformer of DAE through complementary hydrogen bonds. Atomic force microscopy, UV/Vis spectroscopy, and molecular modeling revealed that our DAE and PBI building blocks coassembled in nonpolar solvent to form well-defined helical nanofibers featuring J-type dimers of PBI dyes. Upon irradiating the coassembly solution with UV and visible light in turn, a reversible morphology change between nanofibers and nanoparticles was observed. This system involves the generation of a new self-assembly pathway by means of photocontrol.

- Temperature-Responsive Microgel Films as Reversible Carbon Dioxide Absorbents in Wet Environment
  Yue, M.; Hoshino, Y.; Ohshiro, Y.; Imamura, K.; Miura, Y. *Angew. Chem. Int. Ed.* **2014**, *53*, 2654–2657.
  Abstract:

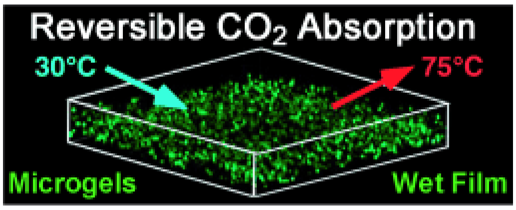

Hydrogel films composed of temperature-responsive microgel particles (GPs) containing amine groups work as stimuli-responsive carbon dioxide absorbent with a high capacity of approximately 1.7 mmol g^{-1}. Although the dried films did not show significant absorption, the reversible absorption capacity dramatically increased by adding a small amount of water (1 mL g^{-1}). The absorption capacity was independent of the amount of added water beyond 1 mL g^{-1}, demonstrating that the GP films can readily be used under wet conditions. The amount of CO_2 absorbed by the GP films was proportional to their thickness up to 200–300 µm (maximum capacity of about 2 L m^{-2}). Furthermore, the films consisting of GPs showed faster and greater absorption and desorption of CO_2 than that of monolithic hydrogel films. These results indicated the importance of a fast stimulus response rate of the films that are composed of GPs in order to achieve long-range and fast diffusion of bicarbonate ions. Our study revealed the potential of stimuli-responsive GP films as energy-efficient absorbents to sequester CO_2 from high-humidity exhaust gases.

- Naphthylamine–Rhodamine-Based Ratiometric Fluorescent Probe for the Determination of Pd^{2+} Ions

  Sun, S.; Qiao, B.; Jiang, N.; Wang, J.; Zhang, S.; Peng, X. *Org. Lett.* **2014,** *16*, 1132-1135.

  Abstract:

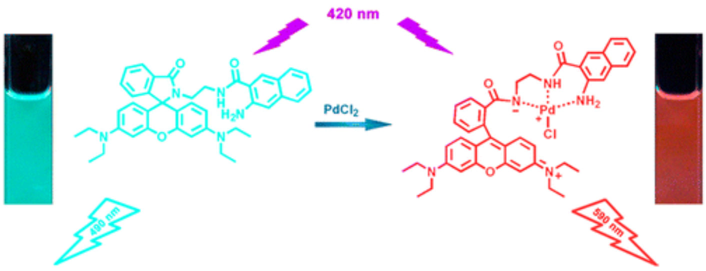

A naphthylamine–rhodamine hybrid ratiometric and colorimetric fluorescent probe (**RN**) was designed and synthesized. **RN** can identify Pd^{2+} ions with high selectivity and sensitivity. Furthermore, the probe can be used to monitor Pd^{2+} ions in live mice by fluorescence imaging.

- Preparation and Characterization of a Halogen-Bonded Shape-Persistent Chiral Alleno-acetylenic Inclusion Complex.

  Castro-Fernández, S.; Lahoz, I. R.; Llamas-Saiz, A. L.; Alonso-Gómez, J. L.; Cid, M.-M.; Navarro-Vázquez, A. *Org. Lett.* **2014,** *16*, 1136-1139.

  Abstract:

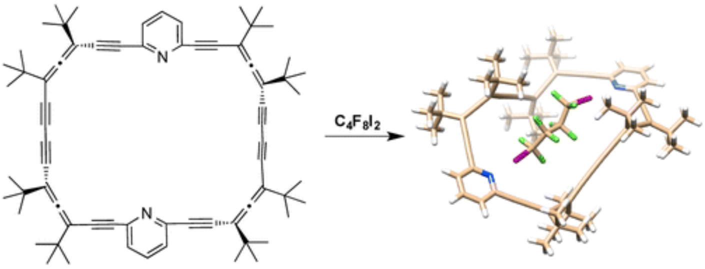

A chiral bidentate inclusion complex has been formed by halogen-bond interaction between the pyridyl moieties of a pyridoallenoacetylenic host and octafluorodiiodobutane. X-ray crystallography showed that the guest adopts a chiral conformation inside the molecular channels formed by stacking of the host units. A 10 ppm shielding of the ^{15}N NMR resonance for the pyridil units provided evidence of the formation of the halogen-bond complex in solution.

- High-Performance Electrocatalysts for Oxygen Reduction Derived from Cobalt Porphyrin-Based Conjugated Mesoporous Polymers

  Wu, Z.-S.; Chen, L.; Liu, J.; Parvez, K.; Liang, H.; Shu, J.; Sachdev, H.; Graf, R.; Feng, X.; Müllen, K. *Adv. Mater.* **2014**, *26*, 1450–1455.

  Abstract:

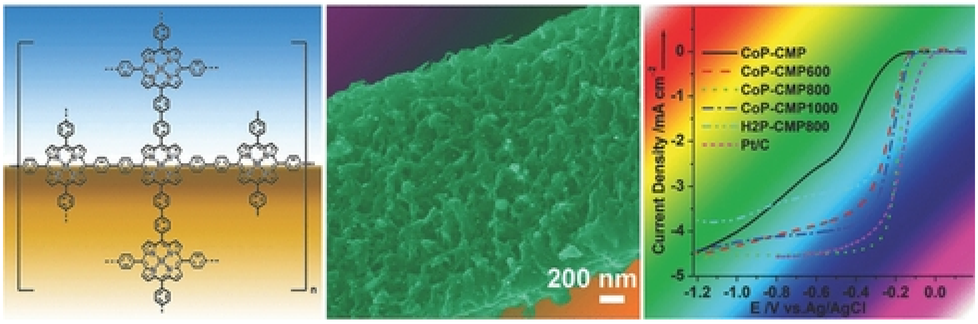

A cobalt-nitrogen-doped porous carbon that exhibits a ribbon-shape morphology, high surface area, mesoporous structure, and high nitrogen and cobalt content is fabricated for high-performance self-supported oxygen reduction electrocatalytsts through template-free pyrolysis of cobalt porphyrin-based conjugated mesoporous polymer frameworks.

- Robust Self-Healing Host–Guest Gels from Magnetocaloric Radical Polymerization
  Yu, C.; Wang, C.-F.; Chen, S. *Adv. Funct. Mater.* **2014**, *24*, 1235–1242.
  Abstract:

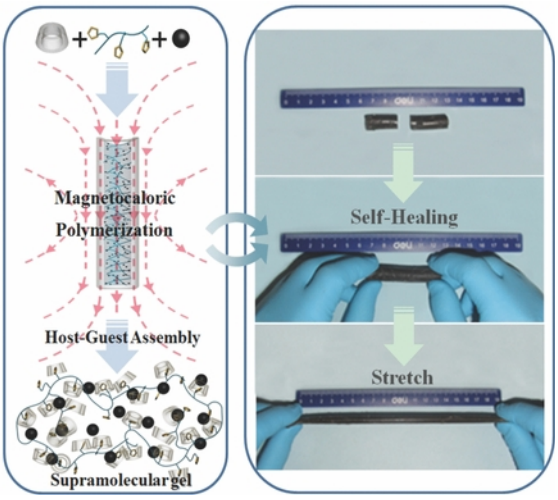

Given the increasing environmental and energy issues, materials with the ability to repair themselves following damage are highly desirable because this self-healing property can prolong the lifespan of materials and reduce replacement costs. Host–guest assemblies are a powerful approach to create supramolecular materials with versatile functions. Here, a new mode of radical polymerization is demonstrated which is achieved via magnetocaloric effect to fabricate novel host–guest supramolecular gels within 5 min. The resulting gels can repair themselves spontaneously when damaged, without the assistance of any external stimuli, and possess great mechanical strength. Moreover, the Fe_3O_4-doped supramolecular gels show accelerated self-healing (from 24 h to 3 h) under an applied magnetic field, which is attributed to the synergy between host–guest healing and a magnetocaloric effect. This strategy might open a promising avenue for accelerating the use of host–guest assemblies to rapidly build robust materials.

- Self-Assembly of a Highly Organized, Hexameric Supramolecular Architecture: Formation, Structure and Properties
  Schaeffer, G.; Fuhr, O.; Fenske, D.; Lehn, J.-M. *Chem. Eur. J.* **2014**, *20*, 179–186.
  Abstract:

Two derivatives, $^{3}\mathbf{L}$ and $^{9}\mathbf{L}$, of a ditopic, multiply hydrogen-bonding molecule, known for more than a decade, have been found, in the solid state as well as in solvents of low polarity at room temperature, to exist not as monomers, but to undergo a remarkable self-assembly into a complex supramolecular species. The solid-state molecular structure of $^{3}\mathbf{L}$, determined by single-crystal X-ray crystallography, revealed that it forms a highly organized hexameric entity $^{3}\mathbf{L}_6$ with a capsular shape, resulting from the interlocking of two sets of three monomolecular components, linked through hydrogen-bonding interactions. The complicated ^{1}H NMR spectra observed in *o*-dichlorobenzene (*o*-DCB) for $^{3}\mathbf{L}$ and $^{9}\mathbf{L}$ are consistent with the presence of a hexamer of D_3 symmetry in both cases. DOSY measurements confirm the hexameric constitution in solution. In contrast, in a hydrogen-bond-disrupting solvent, such as DMSO, the ^{1}H NMR spectra are very simple and consistent with the presence of isolated monomers only. Extensive temperature-dependent ^{1}H NMR studies in *o*-DCB showed that the $\mathbf{L}_6$ species dissociated progressively into the monomeric unit on increasing th temperature, up to complete dissociation at about 90 °C. The coexistence of the hexamer and the monomer indicated that exchange was slow on the NMR timescale. Remarkably, no species other than hexamer and monomer were detected in the equilibrating mixtures. The relative amounts of each entity showed a reversible sigmoidal variation with temperature, indicating that the assembly proceeded with positive cooperativity. A full thermodynamic analysis has been applied to the data.

- Self-Assembly of Three-Dimensional Supramolecular Polymers through Cooperative Tetrathiafulvalene Radical Cation Dimerization
  Tian, J.; Ding, Y.-D.; Zhou, T.-Y.; Zhang, K.-D.; Zhao, X.; Wang, H.; Zhang, D.-W.; Liu, Y.; Li, Z.-T.
  Chem. Eur. J. **2014**, *20*, 575–584.
  <u>Abstract:</u>

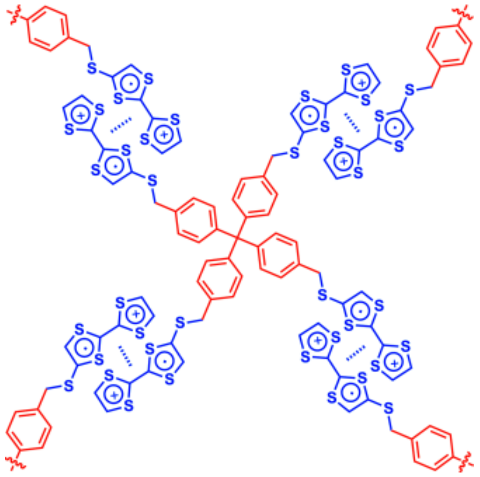

The self-assembly of a new type of three-dimensional (3D) supramolecular polymers from tetrahedral monomers in both organic and aqueous media is described. We have designed and synthesized two tetraphenylmethane derivatives **T1** and **T2**, both of which bear four tetrathiafulvalene (TTF) units. When the TTF units were oxidized to the radical cation $\mathrm{TTF}^{\cdot+}$, their pre-organized tetrahedral arrangement remarkably enhanced their intermolecular dimerization, leading to the formation of new 3D spherical supramolecular polymers. The structure of the supramolecular polymers has been inferred on the basis of UV/Vis absorption, electron paramagnetic resonance, cyclic voltammetry, and dynamic light scattering (DLS) analysis, as well as by comparing these properties with those of the self-assembled structures of mono-, di-, and tritopic control compounds. DLS experiments revealed that the spherical supramolecular polymers had hydrodynamic diameters

of 68 nm for **T1** (75 µM) in acetonitrile and 105 nm for **T2** (75 µM) in water/acetonitrile (1:1). The 3D spherical structures of the supramolecular polymers formed in different solvents were also supported by SEM and AFM experiments.

- Anatase Titania Nanorods as an Intercalation Anode Material for Rechargeable Sodium Batteries
  Kim, K.-T.; Ali, G.; Chung, K. Y.; Yoon, C. S.; Yashiro, H.; Sun, Y.-K.; Lu, J.; Amine, K.; Myung, S.-T. *Nano Lett.* **2014**, *14*, 416–422.
  Abstract:

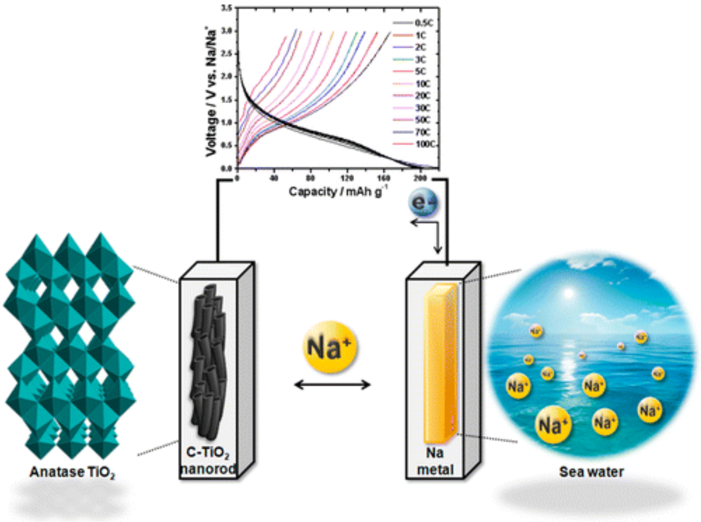

For the first time, we report the electrochemical activity of anatase TiO_2 nanorods in a Na cell. The anatase TiO_2 nanorods were synthesized by a hydrothermal method, and their surfaces were coated by carbon to improve the electric conductivity through carbonization of pitch at 700 °C for 2 h in Ar flow. The resulting structure does not change before and after the carbon coating, as confirmed by X-ray diffraction (XRD). Transmission electron microscopic images confirm the presence of a carbon coating on the anatase TiO_2 nanorods. In cell tests, anodes of bare and carbon-coated anatase TiO_2 nanorods exhibit stable cycling performance and attain a capacity of about 172 and 193 mAh g^{-1} on the first charge, respectively, in the voltage range of 3–0 V. With the help of the conductive carbon layers, the carbon-coated anatase TiO_2 delivers more capacity at high rates, 104 mAh g^{-1} at the 10 C-rate (3.3 A g^{-1}), 82 mAh g^{-1} at the 30 C-rate (10 A g^{-1}), and 53 mAh g^{-1} at the 100 C-rate (33 A g^{-1}). By contrast, the anode of bare anatase TiO_2 nanorods delivers only about 38 mAh g^{-1} at the 10 C-rate (3.3 A g^{-1}). The excellent cyclability and high-rate capability are the result of a Na^+ insertion and extraction reaction into the host structure coupled with $Ti^{4+/3+}$ redox reaction, as revealed by X-ray absorption spectroscopy.

- Programmable Redox State of the Nickel Ion Chain in DNA
  Chu, H.-L.; Chiu, S.-C.; Sung, C.-F.; Tseng, W.; Chang, Y.-C.; Jian, W.-B.; Chen, Y.-C.; Yuan, C.-J.; Li, H.-Y.; Gu, F. X.; Di Ventra, M.; Chang, C.-C. *Nano Lett.* **2014**, *14*, 1026–1031.
  Abstract:

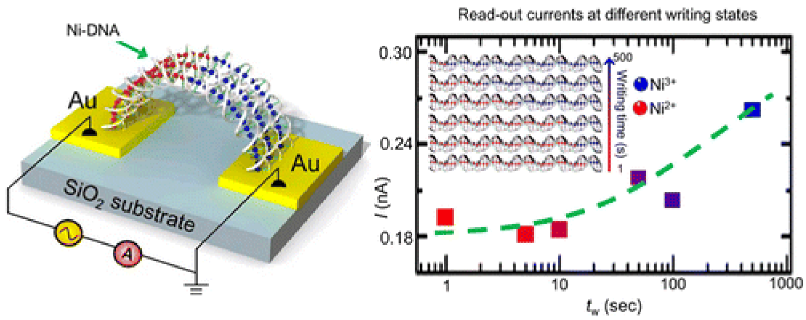

DNA is a nanowire in nature which chelates Ni ions and forms a conducting chain in its base-pairs (Ni-DNA). Each Ni ion in Ni-DNA exhibits low (Ni^{2+}) or high (Ni^{3+}) oxidation state and can be switched sequentially by applying bias voltage with different polarities and writing times. The ratio of low and high oxidation states of Ni ions in Ni-DNA represents a programmable multistate memory system with an added capacitive component, in which multistate information can be written, read, and erased. This study also indicates that the biomolecule-based self-organized nanostructure can be used as a template for nanodevice fabrication.

- Structure–Property Relationship of Pyridoindole-Type Host Materials for High-Efficiency Blue Phosphorescent Organic Light-Emitting Diodes
  Lee, C. W.; Lee, J. Y. *Chem. Mater.* **2014**, *26*, 1616–1621.
  Abstract:

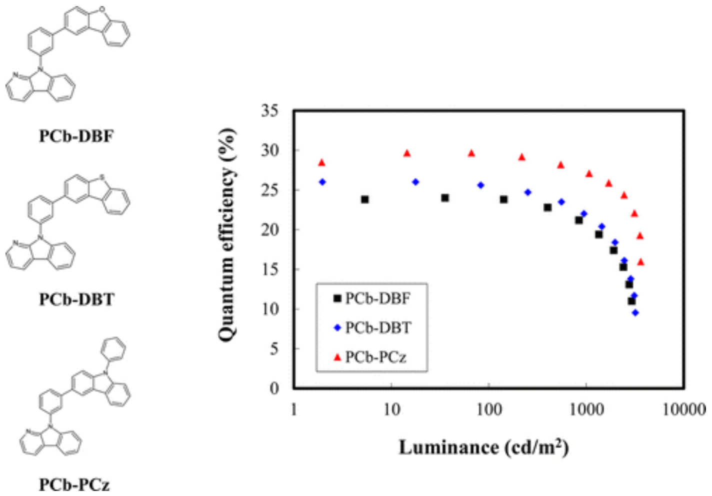

The structure–property relationship of pyridoindole-type host materials for blue phosphorescent organic light-emitting diodes (PHOLEDs) was investigated by synthesizing three pyridoindole derivatives modified with dibenzofuran, dibenzothiophene, and 9-phenylcarbazole. The 9-phenylcarbazole moiety was better than dibenzofuran or dibenzothiophene to manage the energy levels and charge-transport properties of the pyridoindole-derived host materials. The PCb-PCz host with the 9-phenylcarbazole moiety showed balanced charge density in the emitting layer and exhibited a high external quantum efficiency of 29.7% in blue PHOLEDs.

- A star-shaped bipolar host material based on carbazole and dimesitylboron moieties for fabrication of highly efficient red, green and blue electrophosphorescent devices
  Shi, H.; Xin, D.; Dong, X.; Dai, J.-X.; Wu, X.; Miao, Y.; Fang, L.; Wang, H.; Choi, M. M. F. *J. Mater. Chem C* **2014**, *2*, 2160–2168.
  Abstract:

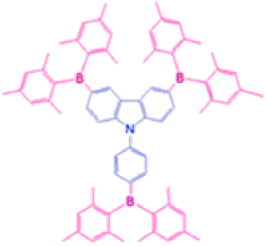

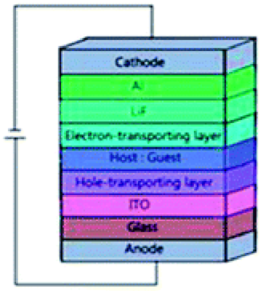

A new bipolar host material based on carbazole and dimesitylboron moieties, 3,6-bis(dimesitylboryl)-9-(4-(dimesitylboryl)phenyl) carbazole (**BDDPC**), has been successfully synthesised and characterised by elemental analysis, nuclear magnetic resonance spectroscopy, mass spectrometry and thermogravimetric analysis. The electrochemical and photophysical properties of **BDDPC** are studied by both experimental and theoretical methods. **BDDPC** exhibits excellent thermal stability (T_d = 234 °C), electrochemical stability, high fluorescence quantum yield (0.95) and high triplet energy (2.83 eV). A red phosphorescent organic light-emitting diode (PhOLED) device comprising **BDDPC** as the host material and $Os(bpftz)_2(PPh_2Me)_2$ as the dopant is fabricated and displays promising electrophosphorescence properties with a turn-on voltage of 3.0 V, a maximum brightness of 12 337 cd m^{-2} and a maximum current efficiency of 11.04 cd A^{-1}. Similarly, **BDDPC** is used to fabricate a green PhOLED device with $Ir(ppy)_2(acac)$ as the dopant, possessing a turn-on voltage of 2.5 V, a maximum brightness of 26 473 cd m^{-2} and a maximum current efficiency of 38.60 cd A^{-1}. Furthermore, a blue PhOLED device with **BDDPC** as the host material and FIrpic as the dopant is fabricated with a turn-on voltage of 3.0 V, a maximum brightness of 7622 cd m^{-2} and a maximum current efficiency of 7.39 cd A^{-1}. It is anticipated that **BDDPC** has great potential in manufacturing PhOLED devices for display or lighting applications.

- How Shape Affects Microtubule and Nanoparticle Assembly
  Stevens, M. J. *Science* **2014,** *343*, 981-982.
  Abstract:

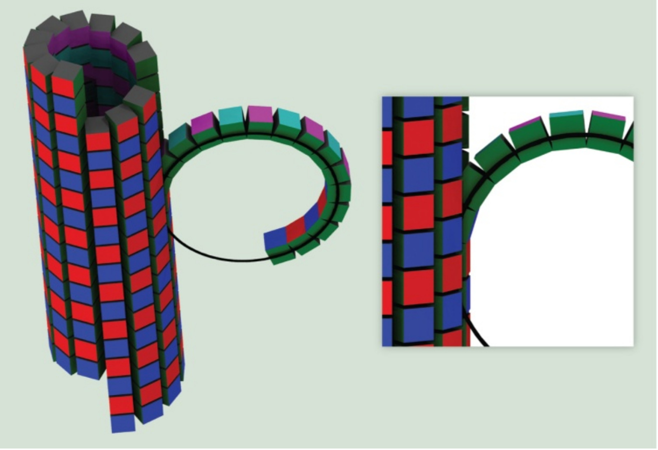

Part of the tantalizing promise of nanoparticles is that they can serve as building blocks of complex systems that could outperform other materials. For example, different structures could form depending on the shape of the nanoparticles. A stimulus, such as a change in temperature or the addition of a small molecule, that changes nanoparticle shape could create a new structure with a different function. Nature provides a large example set of nanoparticles in the form of proteins, which can be studied to gain insight into shape-dependent assembly. In a recent paper, Ojeda-Lopez *et al.* describe a new shape-changing mechanism that dramatically alters how a protein system assembles. The α–β tubulin dimer naturally polymerizes to form microtubules. The authors discovered that adding a highly charged small molecule, spermine, causes a shape transformation. The tubules assemble within an inverted structure compared to that of the original microtubules.

- How force unfolding differs from chemical denaturation
  Stirnemann, G.; Kang, S.-G.; Zhou, R.; Berne, B. J. *Proc. Natl. Acad. Sci. U. S. A.* **2014,** *111*, 3413-3418.
  Abstract:

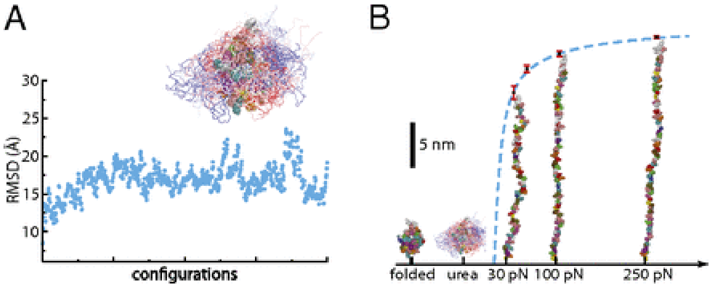

Proteins can be unfolded either chemically by denaturing agents (such as urea) or by mechanical force (such as optical tweezers). If these two methods produce quite different unfolded structures, the course of the subsequent protein refolding when these agents are removed will be quite different. Our computer simulations show that the respective unfolded states are indeed very different, being fully extended under force, with no contacts, and partially extended in urea with many nonnative contacts. Understanding these differences is crucial because such configurations serve as starting points for different single-molecule experimental studies of protein folding. These differences can affect both the folding mechanism and the kinetics observed, leading to very different interpretations.